ON-LINE LASER CLEANING OF SKIN-PASS ROLLS

G. Symens – Centre de Recherches Métallurgiques ASBL, Belgium
S. Kiakidis – Tata Steel Nederland Technology B.V., The Netherlands
M. Mertens – P-Laser, Belgium

This paper presents the first results (at month 12) of the EU RFCS project OLACSKIN (Grant Agreement Number 101156458), which aims to demonstrate an innovative laser-based cleaning solution for zinc staining and zinc fouling at the skin-pass mill.

After outlining the project context and objectives, the discussion will focus on the early insights related to the characterisation of the work rolls contamination and the first results obtained on zinc removal by laser.

If successful, this project will result in a yearly reduction of: 30.000 m³ of wastewater, 40 m³ of detergent, and a significant amount of energy (about 18 kW continuously for high-pressure pumps).
In addition to significantly reducing environmental impact, offering a more sustainable and eco-friendly skin-pass operation, it will also open up new opportunities in 'dry skin-pass rolling' and could offer a substitute solution for CrVI coating of rolls.

KEYWORDS: LASER CLEANING – DRY SKIN-PASS – GALVANISING – INSPECTION SYSTEM

INTRODUCTION:

Hot dip galvanized steel products, especially for the automotive industry, have high requirements on the steel surface appearance as this directly affects the visual appearance of the final product (e.g. painted car body). The zinc coated steel surface requires a fine surface texture (roughness) which is made during so called “skin-pass rolling” where the surface texture from skin-pass work rolls (WR) is imprinted in the steel strip surface while a final steel thickness reduction of 0.5-2% is applied to enhance the steel mechanical properties. Strict production measures and quality control measures have been implemented in the production processes to assure the high steel surface quality. Nevertheless, surface quality related issues are responsible for 70% of the quality control rejects. [1], [2], [3], [4], [5], [6], [7], [8], [12]

Two problems occur during skin-pass rolling which negatively affect the steel strip surface quality:

1. **Zn fouling**: homogeneous Zn pollution on WR

Change of the work roll surface texture during a 2-3 day rolling campaign. This change in work roll surface texture strongly affects the texture which can be imprinted in the zinc coated steel strip and is partly caused by microscopic wear and partly by zinc fouling the work roll texture, i.e. zinc from the coated steel strip gradually fills the work roll texture. 30-40% of the quality control rejections are related to zinc fouling. [8]

2. **Zn staining**: localised Zn pollution on WR

Non-homogeneous work roll surface texture due to zinc (and dirt) staining resulting in flat-spots in the zinc coated steel strip. Although the zinc transfer from the coated steel strip to the work roll is a slow process, it is only picked up by the camera inspection systems during product quality control when the staining has passed a certain threshold. Excessive staining causes 20% of the quality control rejections and in 10-20% of the cases can only be solved by replacing skin-pass rolls; causing process interruption and additional cost for skin-pass roll refurbishment.
The current “state-of-the-art” solution to both problems is a washing system which uses high volumes of water

with detergent. The washing system consists of low-pressure sprays which wet the steel strip to minimize zinc fouling and high pressure (150 bar) jets which provide additional cleaning of the work rolls. [10]

Although the water jet system enables less zinc staining than old fashion brushing systems, it cannot always maintain the required level of <1% zinc, generates large amounts of 30000 m³ (waste) water per skin pass mill per year, and consumes significant amount of energy (about 18kW continuously for high pressure pumps). While the water slightly reduces rolling forces during skin-pass rolling, the use of water is unfavourable as it negatively affects the surface texture transfer from the skin-pass rolls to the strip and disturbs visual inspection systems to detect staining in an early stage. [12], [13], [14]

In the frame of an European funded project (OLACSKIN, Grant Agreement Number 101156458), a solution will be developed based on:

- A **laser system** and optics which enable in-situ removal of zinc from a steel skin-pass roll in a hot dip galvanizing line.
- A **visual control system** which monitors the skin-pass roll surface and uses predictive (artificial intelligence based) models to make effective use of the laser power available. This includes both the removal of zinc to prevent zinc fouling and identification of spots where staining starts to occur to enable preventive cleaning actions and zero-defect production.
- **Cleaning process parameters** which enable efficient zinc removal without negatively affecting the hardness (wear resistance) of the skin-pass roll.

In order to reach all project objectives, the project comprises the following phases and areas of investigation:

1. **Preparation phase**

During this first phase, the 3 main objectives will be realized in parallel: "In depth analysis of zinc fouling and staining", "Setting-up on-line measurement systems" and "Tuning of the laser system". So, in this phase each component is tuned separately.

2. **Tuning phase**

This phase is the key one that will combine the first phase results and allow to integrate the main project components into the demonstration phase. So, in this phase all components are tuned as a single assembly.

3. **Demonstration phase**

This is the final step of the technical part of the project, the goal is to demonstrate that the solution is working and to quantify the benefits in comparison with the wet cleaning system.

This paper will give an overview of the main findings and lessons learned during the completion of most of the Preparation phase, which covers the first 18 months of the project. The discussion will primarily address the characterisation of the work rolls contamination and present the initial results of the laser cleaning solution, mainly for zinc fouling. The next steps of the project will be briefly outlined before drawing preliminary conclusions.

CHARACTERISATION OF THE WORK ROLLS CONTAMINATION:

One of the main objectives of the first phase of the project is to gain a comprehensive understanding of zinc fouling, and to characterize its formation and evolution during rolling campaigns. To this end, several tests were carried out on both industrial and pilot mill WRs to quantify the Zn fouling distribution and rate, which will dictate the necessary speed of the Zn cleaning process. These investigations included a preliminary trial, an industrial trial of 10 WRs, and a pilot mill trial, all performed in facilities of TATA Steel in IJmuiden.

Zinc pollution along the WR width and campaign length effect

Before conducting the main experimental campaign, preliminary trials were performed to establish best practices on Zn fouling measurements. Based on these initial tests, the following key observations were revealed:

The XRF measurements along the WR length exhibit an increased concentration of Zn at the sides of the WR, compared to the central part, see Fig. 1. To shed light on this phenomenon, the width of all strips from the last campaign of the examined WR set were investigated. There are 4 width clusters, reducing progressively from 1500 mm to 1075 mm. These widths are also plotted in Fig. 1, as vertical lines. It is obvious that the area of increased Zn content overlaps with the strips' edges. This behaviour is anticipated also at the main industrial trial, were 10 WRs will be measured, see Fig. 2.

The second goal of the preliminary trial (part 2) was to specify the most efficient Zn etchant, which will be used during all the subsequent trials to investigate the exact amount of Zn deposited on a specific area. Two solvents were examined: HCl (+ inhibitor) and NaOH. The objective in this case is to dissolve the deposited Zn, without damaging the substrate (Cr – plated steel). Evidently, both solutions are able to dissolve Zn successfully, but only NaOH leaves the Cr undamaged. Therefore, it was decided to conduct all subsequent measurement using NaOH as a solvent.

The last objective of the preliminary trial was the investigation of the backup roll influence on Zn fouling. XRF measurements were taken along the body length BUR to quantify any Zn contamination. The measured Zn concentration was negligible, which leads to the conclusion to exclude the effect of the BUR in the rest of the study.

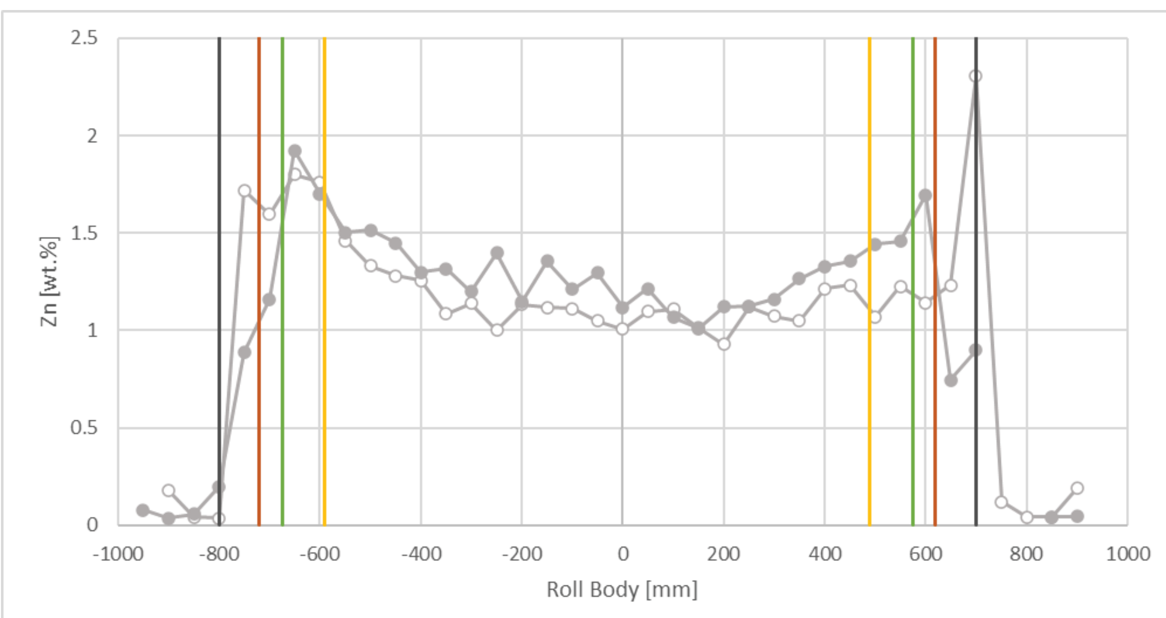

Fig. 1 - XRF measurements (in wt%) along the WR length for 2 skin-pass WRs (top & bottom). The vertical lines indicate the position of the respective strip widths: grey, w > 1450mm; red, 1300 < w < 1450mm; green, 1150 < w < 1300mm; and yellow, w < 1150mm.

After completing the preliminary trial, the main industrial trial started, which included a range of combinations of different WR textures, strip coatings, and rolling lengths, see Tab. 1.

Tab. 1 – Summary of the Zn measurements on industrial work rolls. LR: low WR texture, HR: high WR texture, GI: galvanised iron (regular Zn coating), ZM: Zn coating with increased Mg concentration. WR ID: work roll identification number.

#	WR ID	Roll Position	WR Texture	Strip coating	Rolling Length L [km]
1	159	top	LR	ZM	127
2	160	bot	LR	ZM	127
3	158	top	LR	GI	89
4	172A	top	HR	GI	88
5	161	top	HR	GI	118
6	151	bot	HR	GI	118
7	172B	bot	HR	GI	140
8	174	top	HR	GI	140
9	175	top	LR	ZM	111
10	176	bot	LR	ZM	111

The following observations were made based on results presented in Fig. 2:

- ZM campaigns cause significantly less Zn fouling on the WR surface.
- The Zn fouling distribution along the WR length follows either the “tower bridge” shape observed at the preliminary trial, or it is rather uniform.
- No conclusion can be drawn based on the dataset on the effect of the campaign length. It is assumed that the campaign length differences are either not large enough, or the Zn fouling phenomenon occurs at the early stages of the campaign. This assumption will be investigated further (Effect of process parameters on zinc fouling).
- There are 2 bottom works rolls (172B & 176) which exhibit higher Zn fouling than their top WR counterparts. The reason behind this phenomenon is unknown.
- There is clearly less Zn fouling on the HR WR compared to the LR WR (bottom graph).

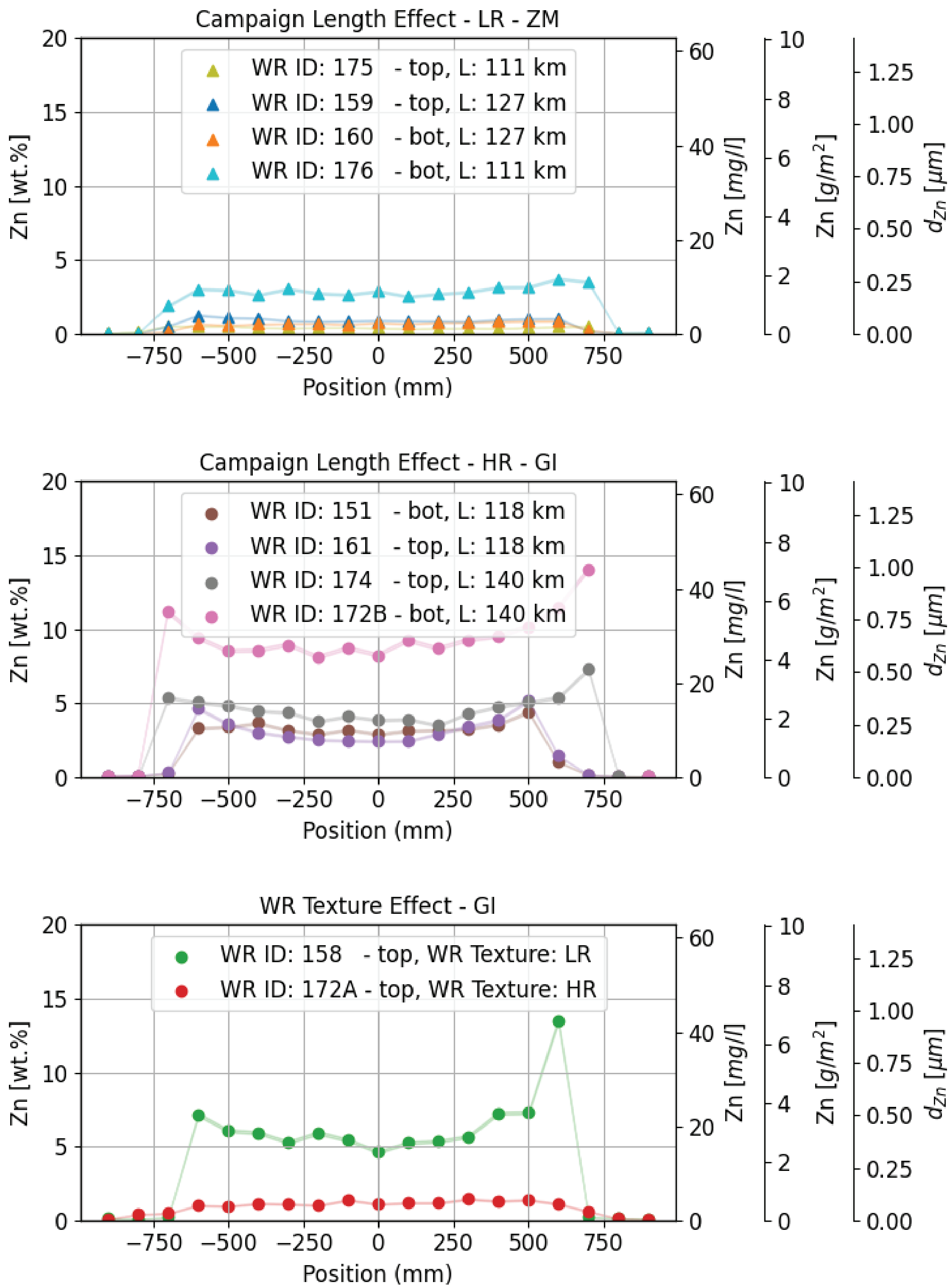

Fig. 2 - XRF measurements across the length of 10 WRs. The WRs are grouped according to their texture and strip coating of their corresponding campaigns.

Top: low WR Texture (**LR**) – Zn/Mg coated (**ZM**) strip

Middle: high WR Texture (**HR**) – galvanized (**GI**) strip

Bottom: WR Texture Effect (**LR**/**HR**) – galvanized (**GI**) strip

Moving on to the chemical analysis, samples (= 100 ml) were etched away from the central[1] part of the WRs and wet chemical analysis was used to determine the Zn concentration [mg/l]. The etched area was approximately 900 mm2, so the following conversion can be done:

$$Zn_{\left[\frac{g}{m^2}\right]} = \frac{V_{sample}}{A_{etched}} 10^{-3} \cdot Zn_{\left[\frac{mg}{l}\right]} \quad [1]$$

where
$V_{sample} = 0.1\ [L]$
$A_{etched} = 900 * 10^{-6}\ [m^2]$

The density of Zn (ρ) is 7140 kg/m^3. Therefore, the Zn concentration can be translated to an <u>average</u> Zn layer thickness, d_{Zn}:

$$d_{Zn_{[\mu m]}} = \frac{1}{\rho} 10^3 \cdot Zn_{\left[\frac{g}{m^2}\right]} \quad [2]$$

The Zn concentration measurement in [mg/l], which was used to estimate the average Zn layer thickness and average Zn fouling speed, cannot be performed in-situ. In contrast, the portable XRF device can be used in a production environment, but it provides the Zn concentration as a (weight) percentage. Fig. 3 illustrates the wet chemical analysis Zn measurements [mg/l] as a function of the XRF measurements [wt.%]. The correlation of the two methods is remarkable. A linear fit can be calculated, intercepting the (0,0) origin, and yielding an $R^2 > 0.99$:

$$Zn_{\left[\frac{mg}{l}\right]} = 3.141 * Zn_{[wt.\%]} \quad [3]$$

As a consequence, the XRF measurements, in combination with [3], may eliminate the need for time consuming wet chemical analysis to determine the deposited Zn.

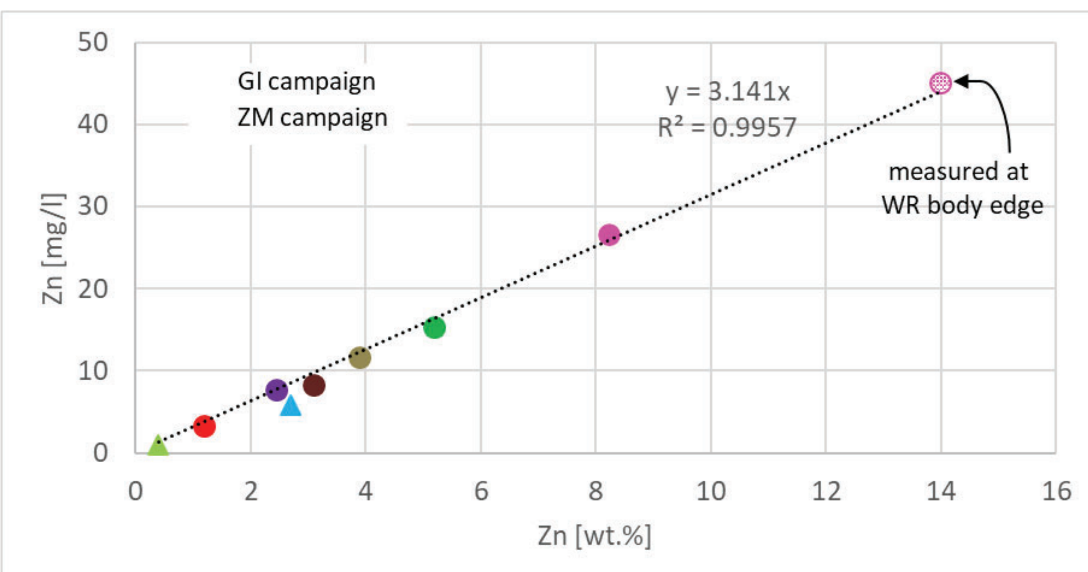

Fig. 3 - Zn concentration in [wt.%], measured by the portable XRF, against the Zn concentration in [mg/l] measured at the etched away samples.

[1] All samples were extracted from the central part of the WRs, except for WR ID = 172B, where samples were taken from both the centre and the edge.

Surface Topography

The 3D topographies of 3 representative cases are illustrated in Fig. 4 (GI campaigns). The following observations are noted:

- At both LR and HR WRs, Zn fouling is present on the worn surface roughness peaks. This behaviour is counter-intuitive because it was expected that Zn would firstly fill the valleys of the surface topography and then the peaks.

- The highest Zn built up is observed on the topography peaks, and on the small valleys that are already elevated compared to the rest of the sample.

- The Zn layer thickness at the GI campaigns may reach up to 10 μm at peak points. There are agglomerations of Zn with an average height of 5 μm, while the rest of the surface is covered with a thin layer of Zn, which is below 2 μm.

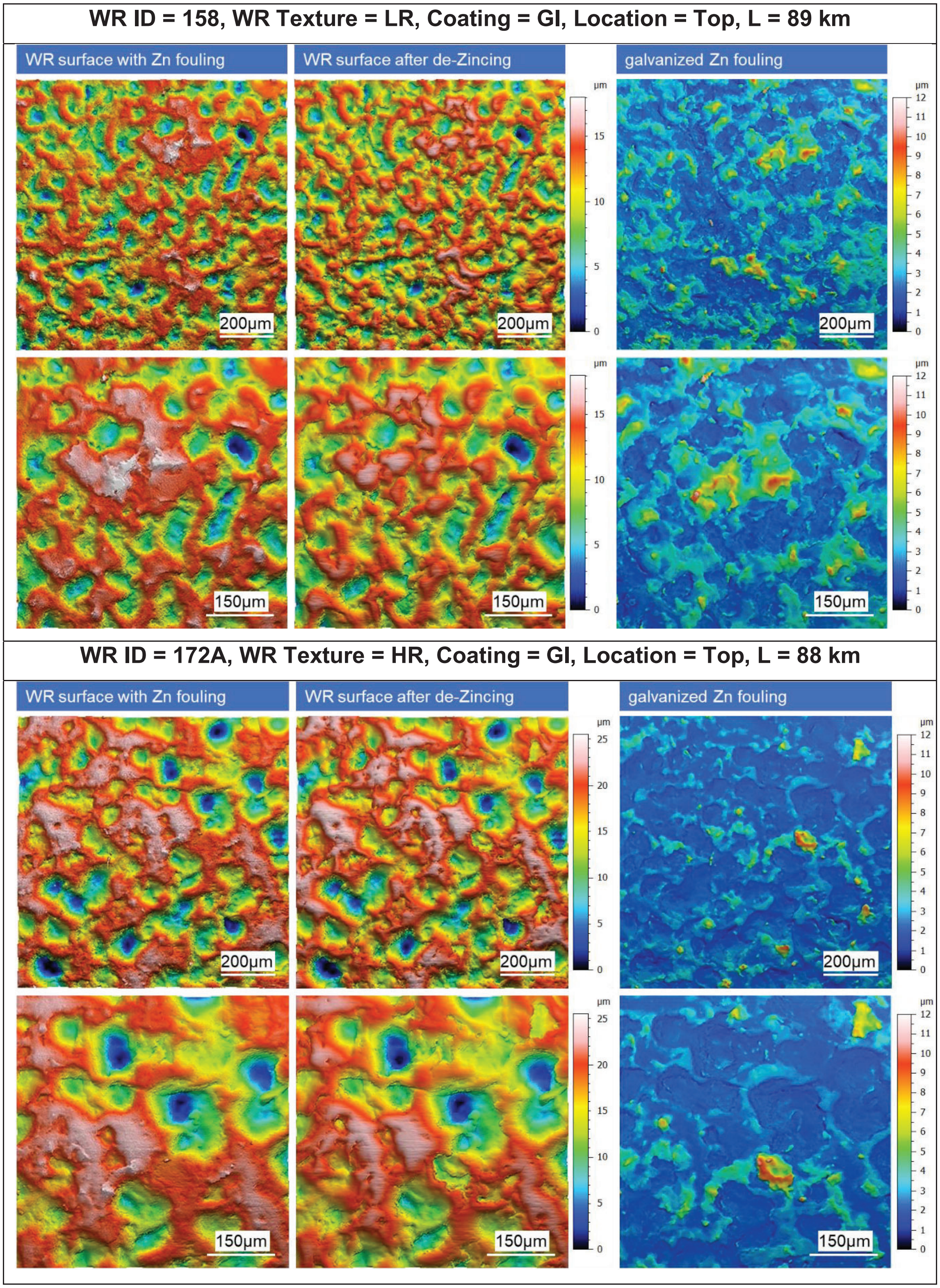

Fig. 4 – Surface topography measured by confocal microscopy for 2 different WRs with GI campaigns. In each WR there are results in 2 magnifications (scale: 150 & 200 µm), before (left) and after de-Zincing (middle). The right figure illustrates the heigh difference between the original (left) and the de-Zinced surface (middle).

Effect of process parameters on zinc fouling

A pilot mill trial was conducted to primarily assess the impact of process parameters on zinc fouling. During this trial, 13 galvanized steel strips were temper rolled under a variety of process conditions. A common low-carbon steel grade was chosen, and each strip had the following geometrical characteristics:

- Width = 150 mm
- Thickness = 2 mm
- Length = 300 – 350 m
- Zn coating thickness = 50 g/m2 per side

Concerning the WRs, two sets have been used: with and without Cr-plating, representing the present and the future[2] situation, respectively. In order to investigate the effect of WR roughness on the Zn fouling phenomenon, each WR set consisted of a low roughness top WR (LR), and a high roughness bottom WR (HR), see Tab. 2.

Tab. 2 – Characteristics of each work rolls (WR) set. EDT: Electro Discharge Texturing.

Set	Position	EDT	Cr – Plated	Diameter
1	Top	Ra = 2.71 µm	No	400 mm
	Bottom	Ra = 4.36 µm	No	400 mm
2	Top	Ra = 2.71 µm	Yes	400 mm
	Bottom	Ra = 4.14 µm	Yes	400 mm

The effect of 6 process parameters was investigated, namely:

1. *Rolling Length*
2. *Rolling Force*
3. *Slip*
4. *Speed*
5. *Cr-plating of WRs*
6. *Detergent usage*

Unfortunately, there is no clear connection between the examined process parameters (except Rolling Length) and the XRF measurements. Therefore, focusing on the XRF results along the rolling length:

- At the Cr plated WR there is a clear difference between the LR (top) WR and the HR (bottom) WR.

- The spread of the measurement is significant, hindering the calculation of an accurate Zn fouling buildup model over the rolling length. The root cause of the spread is the presence (or absence) of large Zn particles at the exact location of the XRF measurement. These are loose Zn particles that create Zn stains on the surface and affect the quantification of the Zn fouling contamination (which is the uniform pickup of Zn on the WRs).

- At the non-Cr plated LR WR, the Zn fouling seems to reach a stable value even after 79 WR revolutions (= 100m of rolling length). The situation is different for the HR WR, where the high spread does not allow for safe conclusions. The trend of the Zn fouling for the HR WR seems even negative. This behaviour is attributed either to the high spread of the XRF measurements, or to the effect of WR wear, which reduces the WR roughness and hinders the Zn pick up.

[2] Ban of Cr-VI process due to REACH legislation

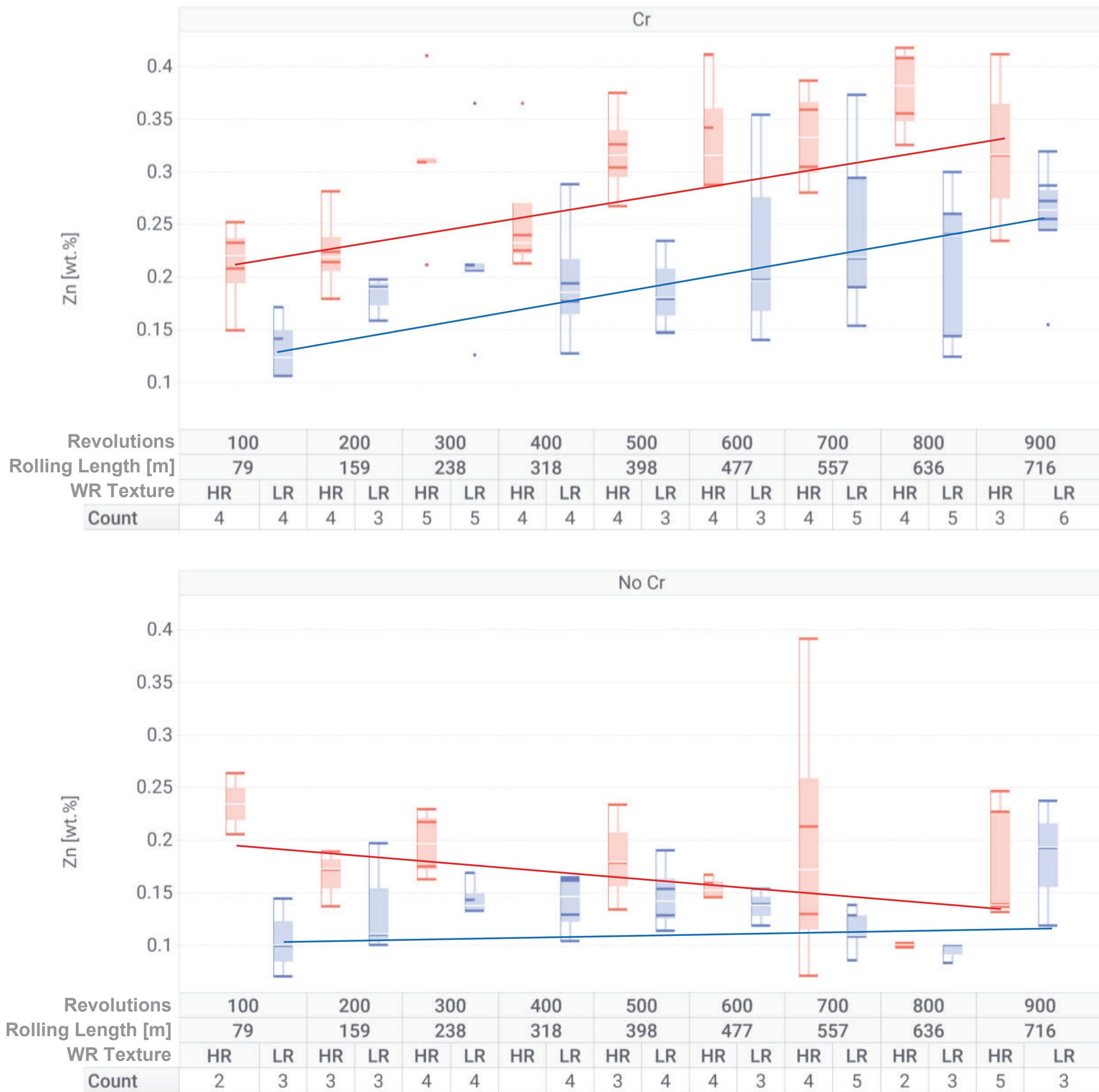

Fig. 5 – Box-plots of the XRF results along the first 900 m of rolling. The measurements concern the first 3 strips (=300 m/strip), rolled with Cr-plated WRs (top) and non-Cr plated WRs (bottom). Box-plot features: (a) median value = white horizontal line, (b) interquartile range = box, (c) min/max values = whiskers, (d) distribution of measurements = non-transparent horizontal lines, (e) number of measurements per boxplot = “count”.

Fig. 5 indicates that the Zn fouling is happening at the early stages of the rolling process. Unfortunately, we don't have Zn measurements before 100 m (=79 WR revolutions). As an alternative, Fig. 6 focuses on the calculation of the Zn fouling speed based on the maximum Zn measurement at 79 revolutions (worst-case scenario), and assuming a linear Zn build-up rate (constant slope). The results of the Zn fouling calculations are presented in Tab. 3.

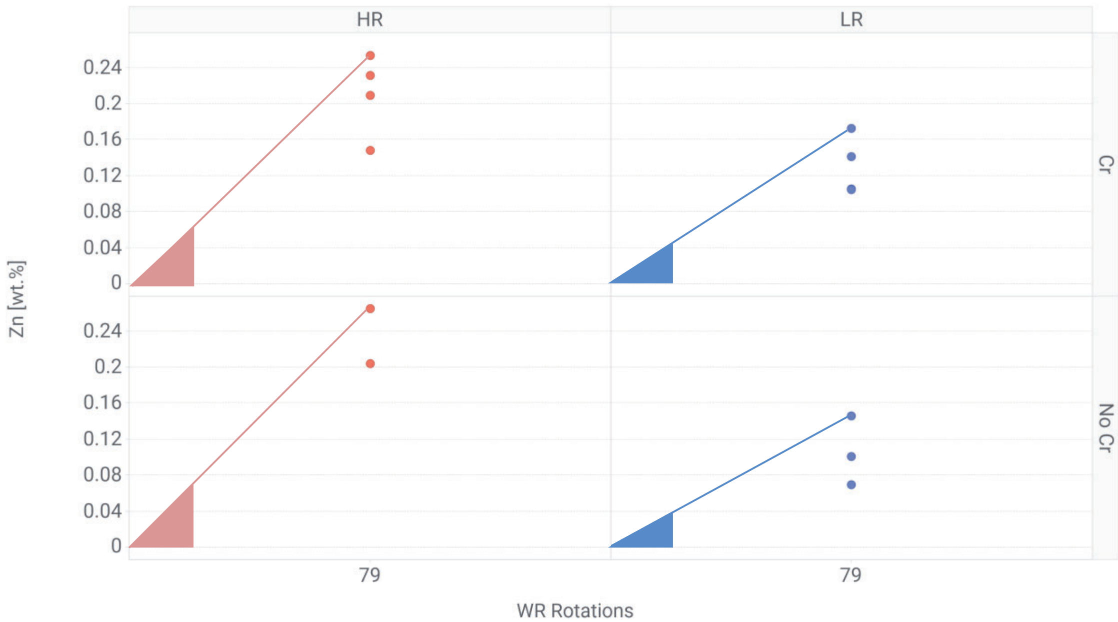

Fig. 6 – Zoomed in version of Fig. 5, focusing on XRF measured Zn (in [wt.%]) at the first 79 WR rotations.

Tab. 3 - Translation of the maximum measured Zn concentration at the first 79 WR rotations in different units. dZn= Zn layer thickness, v = Zn fouling speed.

WR Plating	WR Texture	max Zn [wt.%] @ 79 rev.	Zn [mg/l]	Zn [g/m2]	dZn [µm]	v [nm/rev.]
Cr	LR	0.17	0.543	0.060	0.008	**0.107**
	HR	0.25	0.795	0.088	0.012	**0.157**
Non-Cr	LR	0.15	0.457	0.051	0.007	**0.090**
	HR	0.26	0.832	0.092	0.013	**0.164**

Roughness measurements were also performed; however the results are less relevant within the context of this work, and they are not presented in this paper. Nevertheless, two notable observations were made:

- All three roughness characteristics exhibit a sudden drop at the first measurement (79 WR measurements).
- The roughness skewness (Rsk) drops continuously over the length of the trial, shifting from positive (more peaks) to negative (more valleys) values.

Synthesis of the results

To conclude this part of the study, the main findings of the Zn fouling investigation can be outlined as follows:

Finding 1: Zn fouling distribution across WR length
Based on the industrial WR trials, Zn concentration usually exhibits a "tower bridge" distribution across the WR length. The assumed mechanism behind this behaviour is the following:

- The central part of the WR is constantly in contact with a strip (regardless of strip width). In contrast, the side parts of the roll body are in contact only with the wider strips.
- It could be intuitive that higher Zn concentration would be observed at the roll center due to the constant contact with the strip. However, the constant contact with the strip has an negative effect on the WR wear. As a consequence, the WR roughness drops at the center and the WR cannot pick up Zn easily.
- At the sides, the WR retains great part of its original (ground) roughness, due to lack of contact with the more narrow strips. Therefore, at the side areas the WR can get more excessive Zn fouling.

Finding 2: Zn fouling distribution over the coil length

- Based on the pilot-mill trials, the Zn fouling is happening at the early stages of rolling. Then it reaches gradually a plateau which is maintained to the end of campaign. Therefore the critical Zn fouling speed, which is connected to the Zn cleaning requirements, is calculated based on the Zn fouling measurements at the first 100 m of rolling (=79 revolutions) of the pilot mill trial. For Cr-plated WR with LR texture $v_{Zn} = 0.107\ nm/rev$, and with HR texture $v_{Zn} = 0.157\ nm/rev$. The corresponding speeds for non Cr-plated rolls are $v_{Zn} = 0.090$ and $v_{Zn} = 0.164\ nm/rev$, for LR and HR respectively. Note that the calculated average Zn fouling speed based on the industrial WR measurements is orders of magnitude lower than the speed calculated on the first 79 revolutions of the pilot mill trial. This is a direct consequence of Zn fouling reaching a constant value after a few rolling meters.

Finding 3: Zn fouling morphology

- The results of the confocal microscopy on industrial WR at the EoL indicate that Zn fouling consists of a thin film (<2 μm). However, there are regions of excessive Zn concentration: (a) surface peaks, (a) valleys which are at an elevated area.

Finding 4: WR wear

- Based on the roughness measurements, WR wear is happening at the beginning of rolling, where over time the basic roughness metrics (Ra, Rpc) exhibit a steep drop to a constant value. Note that certain topographical characteristics change more gradually. For example, the ratio between peaks and valleys drifts from positive to negative values (Rsk).

Finding 5: (portable) XRF is a reliable tool to measure Zn fouling

- The ratio between the Zn concentration in [mg/l] and [wt.%] (XRF measurement) is almost constant (=3.141). Therefore, the portable XRF can be used in a production environment to measure in-situ the Zn fouling on the WR, without the need for time-consuming chemical analysis of etched samples. Afterwards, the Zn concentration in [mg/l] can be converted to average Zn layer thickness on the WR surface.

On-line measurement system

As part of the project's objective to implement a closed-loop monitoring system for the WRs cleaning, an on-line inspection system is integrated into the setup. Its purpose is to continuously assess the surface cleanliness of the WR, ensuring optimal cleaning performance and preventing excessive zinc contamination build-up on the roll surface during production campaigns.

During the pilot mill trials, the opportunity was taken to install a first prototype of this on-line inspection system and collect images of the WR surface over time. These images provide valuable information into the evolution of the roll surface condition throughout the trial. The results obtained demonstrated the ability of the on-line inspection system to detect appearing zinc staining on the WR surface but concerning its capability to quantify the zinc fouling level, it still needs to be investigated.

Indeed, as shown on Fig. 7, a large zinc agglomeration is clearly visible and can be easily distinguished from the work roll surface. Except for this type of image, highlighting zinc staining, the remaining images do not reveal any noticeable evolution of the background (WR surface) throughout the campaign.

Nevertheless, this should not necessarily lead to the conclusion that the system is unable to detect zinc fouling, since the sensor was installed during the trial and therefore did not capture images of the work roll surface when it was perfectly clean. According to *Finding 2*, zinc fouling seems to appear at the early stages of rolling, then it reaches gradually a plateau which is maintained to the end of campaign. The absence of noticeable background evolution is therefore likely related to this actual stable condition. Further off-line trials are planned to validate the ability of the inspection system to quantify zinc fouling level.

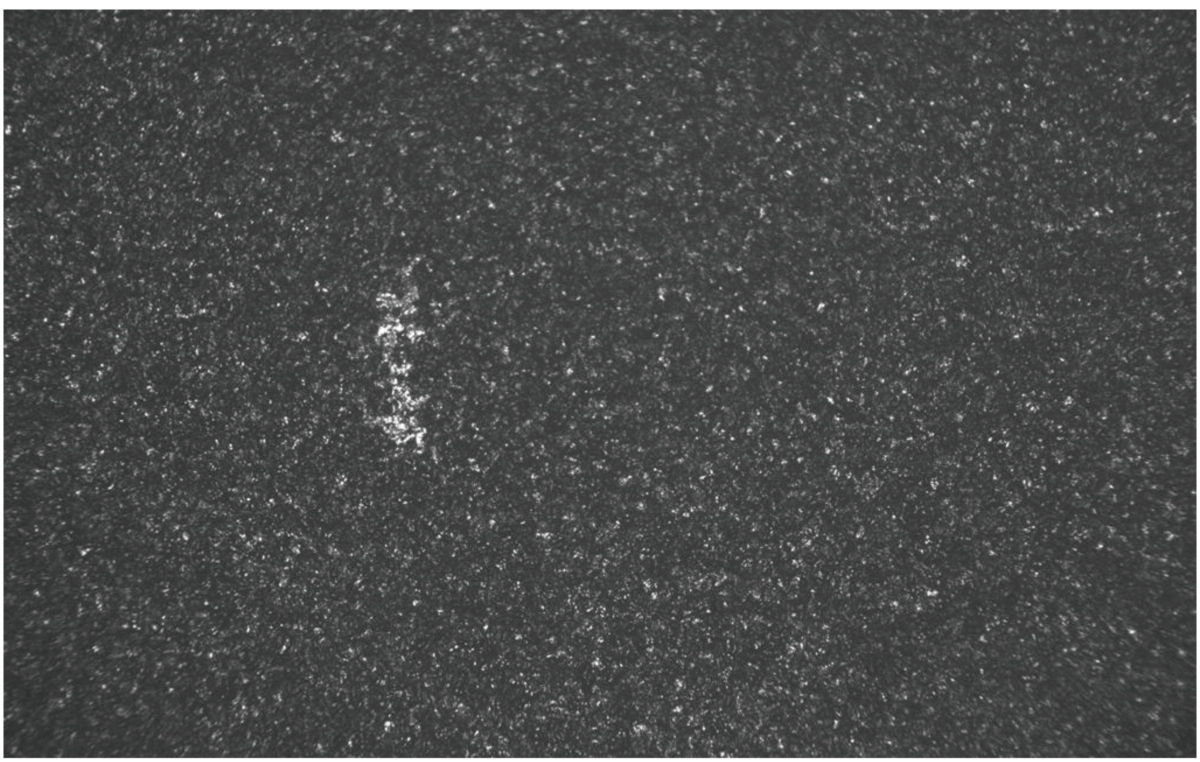

Fig. 7 – Image of a Zn staining taken by the on-line inspection system, configured with a field of view of 7600 μm.

LASER CLEANING OF THE WORK ROLLS:

To explore the practical effectiveness of laser-based cleaning for zinc removal from skin-pass work rolls, a comprehensive matrix of laser cleaning trials was conducted on an end-of-life WR, see Fig. 8. The tests focused on evaluating zinc removal efficiency and preserving roll surface texture under different combinations of pulse energy, pulse duration, filling strategy (uniform vs. random), and number of laser passes.

Experimental parameters

The laser system employed was a P-Laser QF-300 with adjustable pulse energy and pulse duration. In the experimental setup the laser optic was mounted on a fixture, and the work roll was positioned on a motorized rotation beck, see Fig. 8. The key variables explored were:

- **Pulse durations:** Three distinct pulse durations within the nanosecond regime.
- **Pulse energies:** Six different pulse energies ranging from low to moderate values for surface cleaning purposes
- **Number of passes:** 1, 2, 3, 5, 8, 12, 16, 20
- **Filling strategy:** Uniform structured grid and random, multi-pass coverage

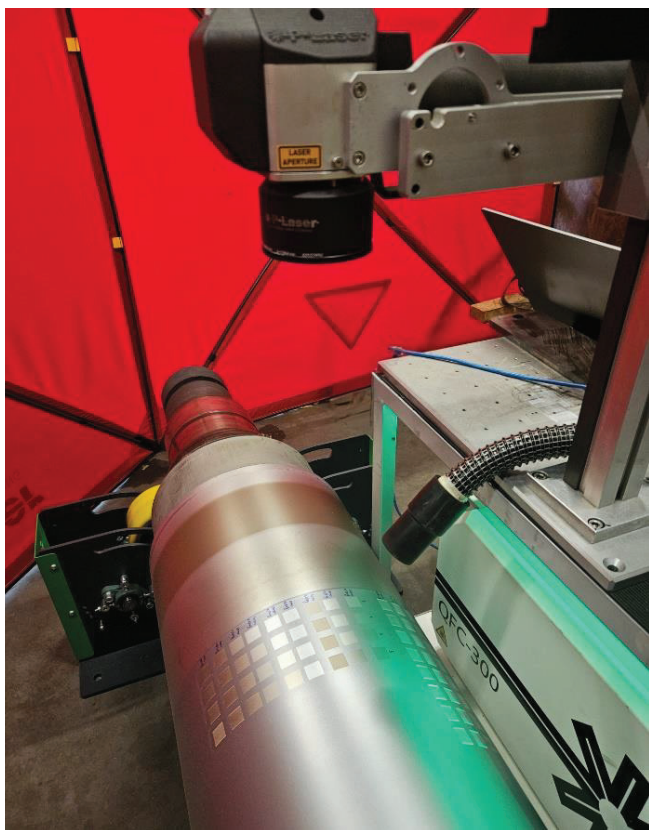

Fig. 8 - Experimental setup with QF-300 laser.

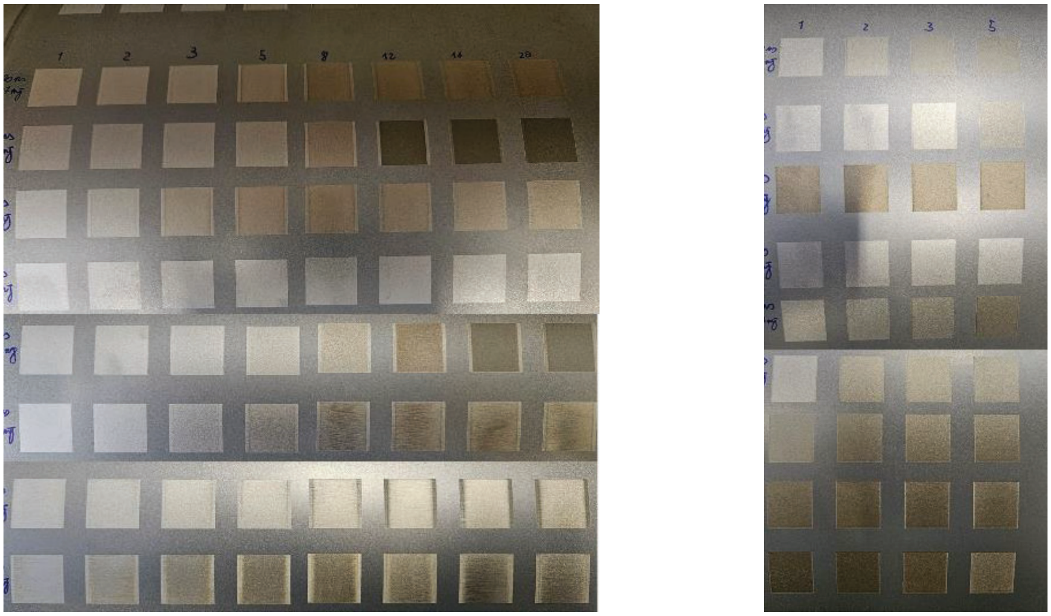

Fig. 9 – Macroscopic view of the Zn cleaning results using different laser settings.

The testing matrix aimed to cover both minimal and aggressive cleaning regimes to identify thresholds for efficient zinc removal and ensure minimal damage or textural alteration. The random filling was included in the test matrix to mimic gradual, randomized cleaning, which is desired in industrial conditions to avoid abrupt changes in the WR (see Fig. 9) that could lead to uneven imprinting or visual defects in the steel strip. Fig. 10 Illustrates the relative positioning of the tested laser settings in terms of pulse energy and pulse duration.

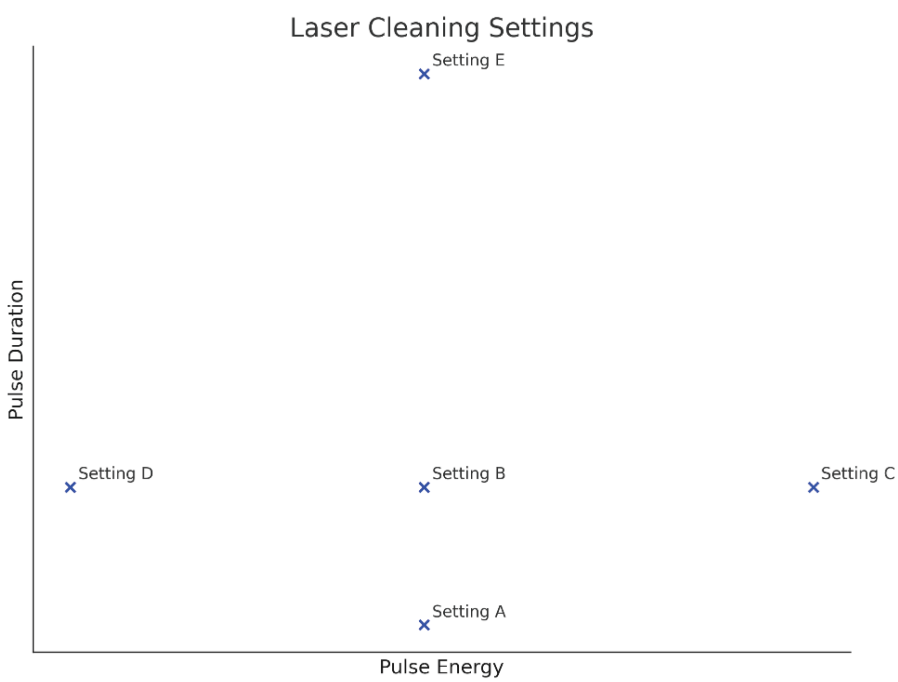

Fig. 10 - Relative positioning of tested laser settings.

Zinc removal performance – XRF results

Zinc removal was assessed using X-ray fluorescence spectroscopy (XRF) on an end-of-life industrial work roll. Initial Zn wt% was on average 0.775%. The Tab. 4 and Tab. 5 below summarize key XRF findings:

Tab. 4 - Uniform Filling – Zn Residuals (wt%)

Setting	Passes = 0	1	2	3	5	20
Setting A	0.775	0	0	0	N.A.	N.A.
Setting B	0.775	0.029	0.021	0	N.A.	N.A.
Setting C	0.775	0	0	0	N.A.	N.A.
Setting D	0.775	0.233	0.088	0	0	0
Setting E	0.775	0.032	0.025	0	0	0

Tab. 5 - Random Filling – Zn Residuals (wt%)

Setting	Passes = 0	1	2	3	5
Setting A	0.775	0	0	0	0
Setting B	0.775	0.021	0	0	0
Setting C	0.775	0	0	0	0
Setting D	0.775	0.231	0.165	0	0
Setting E	0.775	0.026	0.03	0.023	0.019

Key findings

- Zinc is fully removed after 1–2 passes for higher pulse energy settings combined with shorter pulse durations.
- Lower energy settings (e.g., Setting D) require more passes but successfully remove all zinc by 3 passes, without any visible discoloration, suggesting minimal thermal impact and high industrial relevance.
- Random and uniform filling both yield effective and comparable zinc removal results.

Optical microscopy

To verify that no unintended surface modification occurred, optical microscopy was performed on areas treated with setting D. Representative images were taken after both 1 pass and 20 passes to assess the condition of the surface after minimal and extended laser exposure.

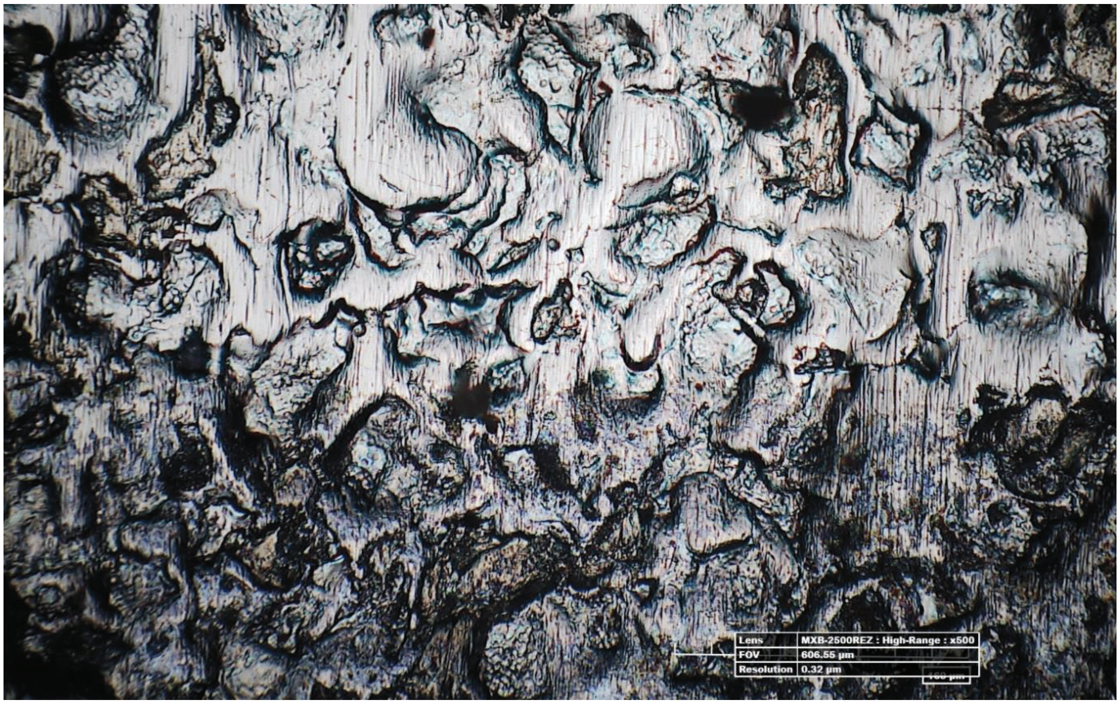

Fig. 11 – Microscope image of Setting D cleaned with 1 pass (top side is cleaned, bottom is untreated).

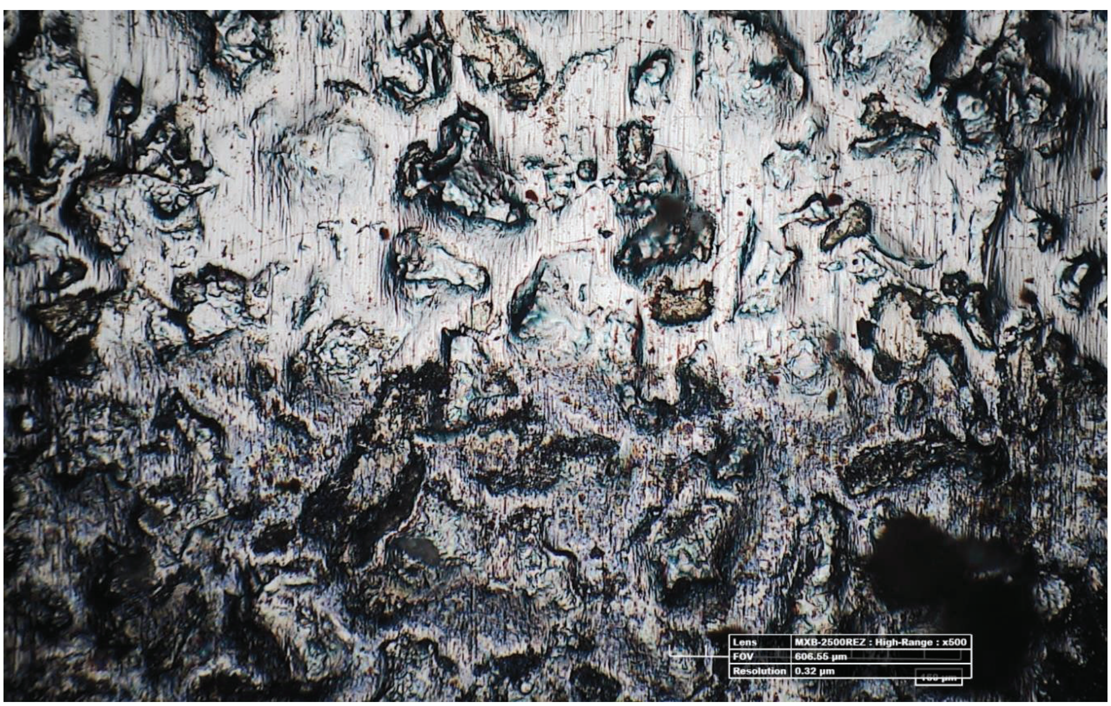

Fig. 12 – Microscope image of Setting D cleaned with 20 passes (top side is cleaned, bottom is untreated).

As shown in Fig. 11 (1 pass) and Fig. 12 (20 passes), the upper portion of each image corresponds to the laser-treated area, while the lower part remains untreated. This side-by-side view allows for a direct visual comparison between the cleaned and uncleaned regions.

The laser-treated zones show no additional damage or discoloration compared to the untreated areas. No signs of surface melting, oxidation, pitting, or microcracking were observed. Even after 20 laser passes, the cleaned surface texture remained well preserved, with no visible alteration beyond the wear already present on the roll.

Roughness measurements

To ensure the cleaning process does not degrade the engineered roll texture, surface roughness was evaluated using mechanical profilometry. The parameters measured included Ra (average roughness) and Rz (mean peak-to-valley height). Roughness measurement results of setting D pulse energy are shown in Tab. 6.

Tab. 6 - Random Filling – Zn Residuals (wt%)

Number of Passes	Ra (µm)	Rz (µm)
1	1.414	8.372
2	1.304	8.011
3	1.386	8.542
5	1.253	7.162
8	1.326	8.049
12	1.310	7.585
16	1.359	8.174
20	1.241	7.681

These results demonstrate that even after 20 passes, both Ra and Rz remain stable. The slight fluctuations are typical for laser–surface interactions and do not indicate any form of damage or excessive smoothing. Combined with optical microscopy, these values reinforce the conclusion that Setting D is non-destructive and effective for laser cleaning of work rolls.

CONCLUSION & NEXT STEPS:

Industrial and pilot trials have provided valuable insights into the nature of zinc fouling. Indeed, these initial results help to identify trends regarding how zinc tends to deposit along the WR width, the typical morphology it takes, and how it evolves throughout the rolling campaign.

This information is essential for guiding the development of both the optical inspection and laser cleaning systems, ensuring that the requirements are properly anticipated in order to achieve effective, consistent WR cleaning and surface homogeneity.

Regarding the first on-line inspection and laser cleaning trials, the results are relatively encouraging. The areas requiring improvement have been clearly identified, which makes it possible to focus future efforts on the most critical aspects.

Moving forward, several key actions are planned to build upon these encouraging results:

- Further investigate the quantification of zinc fouling using the on-line inspection system.
- Finalise the integration of the system, addressing the mechanical constraints within the stand, and validate its performance under rolling conditions.
- Optimize laser cleaning algorithm on a moving target, first on a slow rotation test bench, then at high speed.
- Setting up of a fast rotation bench to synchronise all the equipment and validate the laser cleaning algorithm at operational rolling speeds.

ACKNOWLEDGEMENTS

The Authors of this paper gratefully thank the Commission of the European Communities for the support of this work. The work is funded in part with a grant from the Research Fund for Coal and Steel under research Grant Agreement Number 101156458.

REFERENCES

[1] SMS SIEMAG; skin-pass mills for a perfect finish, W6+7/304E, 1000/01/12

[2] WANG, Chin. J. Mech. Eng. research and development trend of shape control for cold rolling strip, (2017) 30:1248–1261, DOI 10.1007/s10033-017-0163-8

[3] Yoshida et al; A plasticity model describing yield-point phenomena of steels and its application to FE simulation of temper rolling, International Journal of Plasticity 24 (2008) 1792–1818, doi:10.1016/j.ijplas.2008.05.004

[4] D.J. Wentink & al. A generic model for surface texture development, wear and roughness Transfer in skin-pass rolling, Wear 328-329 (2015) 167–176, http://dx.doi.org/10.1016/j.wear.2015.02.015

[5] LEGRAND et al.; ROUGHNESS TRANSFER MODEL BASED ON THE MONTE CARLO METHOD: APPLICATION TO STEEL SHEET TEMPER ROLLING, Technical contribution to the 11th International Rolling Conference, part of the ABM Week 2019, October 1st -3rd, 2019, São Paulo, SP, Brazil.

[6] Wu; A new method for predicting the three-dimensional surface texture transfer in the skin pass rolling of metal strips, Wear 426–427 (2019) 1246–1264, https://doi.org/10.1016/j.wear.2018.12.020

[7] Kijima; Influence of roll radius on contact condition and material deformation in skin-pass rolling of steel strip, Journal of Materials Processing Technology Volume 213, Issue 10, October 2013, Pages 1764-1771, https://doi.org/10.1016/j.jmatprotec.2013.04.011

[8] Nagese et al; The effect of lubricant on microwear of dull rolls in temper rolling by 4hi rolling mill, ISIJ International, Vol. 49 (2009), No. 6, pp. 874-880)

[9] Kainz et al; Finite element modelling of temper rolling with particular emphasis on roughness transfer, ABAQUS Austria Users' Conference, September 27-28, 2005 Kunsthaus Graz

[10] Ogawa et al; Rolling mill roll-cleaning device and cleaning method, WO2012157619A1

[11] Kijima, An experimental investigation on the influence of lubrication on roughness transfer in skin-pass rolling of steel strip, Journal of Materials Processing Technology 225 (2015) 1–8, http://dx.doi.org/10.1016/j.jmatprotec.2015.05.023

[12] KIJIMA; Mechanism of Roughness Profile Transfer in Skin-pass Rolling of Thin Steel Strip, JFE TECHNICAL REPORT No. 24 (Mar. 2019)

[13] Plicht et al; Skin-Pass Rolling of Steel Strip Using Liquid Nitrogen, Conference: Materials Science & Technology Conference At: Detroit, MI (2007)

[14] Heide et al; Steel sheet surfaces with enhanced tactile feel (RFCS STEELTAC), ISSN 1831-9424 (PDF)

[15] Ren et al.; State of the Art in Defect Detection Based on Machine Vision, International Journal of Precision Engineering and Manufacturing-Green Technology volume 9, pages 661–691 (2022)

[16] Zhang et al.; Visual inspection of steel surface defects based on domain adaptation and adaptive convolutional neural network, Mechanical Systems and Signal Processing 153 (2021), 107541

[17] H. Mustafa; (Ultra)Short Pulsed Laser Surface Texturing of Zinc, (2019) PhD thesis [doi: 10.3990/1.9789036548311]

[18] Tata Steel. Patent application [WO2021013939 - METHOD FOR THE REMOVAL OF A COATING FROM A METAL SUBSTRATE BY LASER ABLATION]

[19] Continuous measurement of the surface roughness of a cold-rolled product (US4803374A 1989-02-07)

[20] Method and device for the online determination of the micrometric topography of moving products (EP1806558B1 2012-10-31)

[21] Control of the surface roughness of the steel in temper rolling method (JP2981051B2 1999-11-22)

[22] Apparatus and method for industrial on-line micro-topography and waviness measurements on moving products (EP2517799B1 2014-11-19)

[23] Apparatus for optical measurement of surface properties (DE10151332B4 2007-12-06)

[24] Didarul Amin, Shamim Akhter. Deep Learning-Based Defect Detection System in Steel Sheet Surfaces. Conference: IEEE TENSYMP 2020 At: Dhaka, Bangladesh

[25] Jiangyun Li, Zhenfeng Su, Jiahui Geng, Yixin Yin. Real-time Detection of Steel Strip Surface Defects Based on Improved YOLO Detection Network.

[26] Praveen Damacharla, Achuth Rao M. V., Jordan Ringenberg, Ahmad Y. Javaid. TLU-Net: A Deep Learning Approach for Automatic Steel Surface Defect Detection.

[27] Nico Prappacher, Markus Bullmann, Gunther Bohn, Frank Deinzer, Andreas Linke. Defect Detection on Rolling Element Surface Scans Using Neural Image Segmentation.

[28] Tian Long See et al. Feasibility study and demonstration of cleaning with laser adaptively by novel use of sensors. Conference: 10th CIRP Conference on Photonic Technologies [LANE 2018]

[29] Kruth et al. On-line monitoring and process control in selective laser melting and laser cutting. Conference: 5th Lane Conference, Laser Assisted Net Shape Engineering.